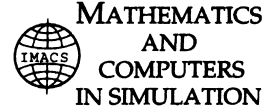




ELSEVIER

Available online at www.sciencedirect.com**SciVerse ScienceDirect**

Mathematics and Computers in Simulation 95 (2013) 137–145

www.elsevier.com/locate/matcom

Original article

Bifurcation analysis of an inductorless chaos generator using 1D piecewise smooth map[☆]

Laura Gardini^{a,*}, Fabio Tramontana^b, Soumitro Banerjee^{c,d}

^a *Università degli Studi di Urbino, Department of Economics, Society, Politics, Via Saffi 42, 61029 Urbino, Italy*

^b *Università degli Studi di Pavia, Department of Economics and Business, Via S. Felice 5, 27100 Pavia, Italy*

^c *Indian Institute of Science Education & Research – Kolkata, Mohanpur Campus, Nadia 741 252, India*

^d *King Abdulaziz University, Jeddah, Saudi Arabia*

Received 3 March 2011; received in revised form 28 May 2012; accepted 30 May 2012

Available online 21 June 2012

Abstract

In this work we investigate the dynamics of a one-dimensional piecewise smooth map, which represents the model of a chaos generator circuit. In a particular (symmetric) case analytic results can be given showing that the chaotic region is wide and robust. In the general model only the border collision bifurcation can be analytically determined. However, the dynamics behave in a similar way, leading effectively to robust chaos.

© 2012 Published by Elsevier B.V. on behalf of IMACS.

Keywords: Chaos generator; Border-collision; Piecewise smooth continuous map

1. Introduction

Many easily implementable circuits have been proposed in the past for the generation of chaotic waveforms meant to be used in different applications. This includes the classic Chua's circuit and its variants [3,4], the Sprott circuits [10], etc. Much study has been directed to the dynamics and bifurcations in such systems.

In view of the possible application of chaos-based communication systems, a new need has arisen for chaos generators that can be completely implemented in VLSI chips. One major hurdle of implementing the usual chaos generators is the inductor, which cannot easily be integrated in microchips. In view of this problem, a new inductorless chaos generator was proposed in [7], and was implemented using a CMOS process. For such a chaotic system which is meant for practical application, it becomes necessary to perform a complete bifurcation analysis, so that its behavior in different parameter regimes can be predicted. This is the purpose of the present paper.

The piecewise smooth one-dimensional map proposed in [7] reduces, in a particular symmetric case, to the piecewise linear one dimensional map which is topologically conjugated with the so-called skew tent map (the continuous piecewise linear one dimensional map in canonical form). Here we use the term 'symmetric' to mean a symmetry in the system configuration where the two resistors in the circuit are of equal value, and not a symmetry in the map

[☆] We thank two anonymous referees for their quite helpful comments.

* Corresponding author.

E-mail addresses: laura.gardini@uniurb.it (L. Gardini), fabio.tramontana@unipv.it (F. Tramontana), soumitro.banerjee@gmail.com (S. Banerjee).

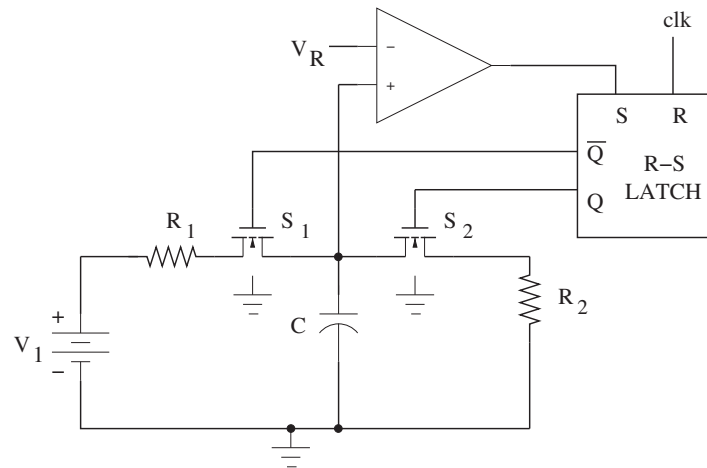


Fig. 1. The inductorless chaos generator.

representing the system. This allows us to completely describe, analytically, the existing dynamics, using the results of the skew tent map. We recall that the preliminary bifurcation analysis of the skew tent map was done in [5,12], and was followed up by more detailed investigations in [2,6,9,11]. In the present paper we use the theory developed in these works, to obtain the parameter domains of different dynamical behaviors of the inductorless chaos generator in the symmetric case. Moreover, also for the generic case the border collision bifurcations leading to the appearance of a pair of k -cycles, $k \geq 3$, are analytically detected. Then we shall see, by numerical evidence, that the sequence of bifurcations occurring in the general model are of the same kind, and lead to robust chaos.

2. The circuit and the mathematical model

We consider the dynamics of a chaos generator shown in Fig. 1 which was designed for easy implementation on a VLSI chip for use in a chaos-based communication system. When the switch S_1 is on, the capacitor C charges up from the battery. When its voltage reaches a reference voltage V_R , S_1 switches off and S_2 switches on. The capacitor discharges through the resistor R_2 . The switch S_1 is again turned on by the positive edge of the free-running clock “clk” with period \bar{T} .

The stroboscopic map of this circuit, as observed at every positive edge of the clock, was derived in [7] as

$$z' = f(z), \quad f(z) = \begin{cases} f_L(z) = 1 - (1 - z)e^{-T_1} & z \leq z_b \\ f_R(z) = \beta e^{-T_2} \left(\frac{1 - z}{1 - \beta} \right)^{T_2/T_1} & z \geq z_b \end{cases} \quad (1)$$

where z is the normalized value of the capacitor voltage at the clock instant v_c/V_1 , $T_1 = \bar{T}/CR_1$, $T_2 = \bar{T}/CR_2$, $\beta = V_R/V_1$ and

$$z_b = 1 - (1 - \beta)e^{T_1}. \quad (2)$$

It was shown, by experiments and via numerical simulations, that robust chaos occurs as a function of all the three parameters $T_1 > 0$, $T_2 > 0$ and $\beta \in (0, 1)$.

In this work we investigate the map in (1). All the possible bifurcations occurring in the symmetric case (for $T_1 = T_2 = T > 0$),¹ are analytically detected in Section 3.1. This leads to a rigorous proof of the numerical results obtained in [7]. In the generic case (for $T_1 \neq T_2$) the existence regions of the so-called maximal cycles are also determined.

We recall that such stable cycles are the most dangerous in the applied context, as destroying the robustness of chaos (which still persists in a set of zero measure, and is structurally unstable). One boundary of the region associated with

¹ We recall that the “symmetric case” is not associated with any symmetry property in the resulting map.

a stable cycle is given by a border collision bifurcation (BCB for short)² curve. The transition to instability occurs via a degenerate flip bifurcation curve in the symmetric case. The bifurcations seem to be of the same kind also in the generic case, as outside these stability regions, we have observed chaotic dynamics. Thus, although supported only by numerical simulations, we have seen that the properties of the piecewise linear model persist in the piecewise smooth one, and we have only robust chaos.

3. Bifurcation analysis

3.1. Symmetric case

To investigate the map in (1) let us first consider the particular case $R_1 = R_2$, which gives

$$T_1 = T_2 = T \tag{3}$$

(and we recall $T > 0$) reducing the parameter space to two dimensions. Consequently, the system reduces to a piecewise-linear map, topologically conjugated with the skew-tent map, whose dynamics are already well known (see [2,5,6,9,11,12]). In fact, with the parameters T and β the map in (1) becomes

$$z' = f(z) = \begin{cases} f_L(z) = 1 - (1 - z)e^{-T} & z \leq z_b \\ f_R(z) = \beta e^{-T} \left(\frac{1 - z}{1 - \beta} \right) & z \geq z_b \end{cases}, \quad z_b = 1 - (1 - \beta)e^T \tag{4}$$

and via the change of coordinate

$$X = z - z_b$$

we have

$$X' = T(X), \quad T(X) = \begin{cases} T_L(X) = aX + B & X \leq 0 \\ T_R(X) = bX + B & X \geq 0 \end{cases} \tag{5}$$

where

$$a = e^{-T}, \quad b = -\frac{\beta e^{-T}}{1 - \beta}, \quad B = \beta - z_b = (1 - \beta)(e^T - 1) \tag{6}$$

Clearly β is a scale parameter.³ Rescaling $x = X/B$ we get:

$$x' = F(x), \quad F(x) = \begin{cases} F_L(x) = ax + 1 & x \leq 0 \\ F_R(x) = bx + 1 & x \geq 0 \end{cases} \tag{7}$$

which is in the form of a skew-tent map, whose properties for $a > 0$ and $b < 0$ are of interest for us (in fact, from (6), $T > 0$ and $\beta \in (0, 1)$, we have $a \in (0, 1)$ and $b < 0$).

In terms of the variable z , the critical point $z = z_b$ is the point of maximum and the absorbing interval⁴ I is given by

$$I = [\beta e^{-T}, \beta]. \tag{8}$$

There exists a unique fixed point (as $T > 0$ and $a = e^{-T} \in (0, 1)$):

$$z^* = \frac{\beta e^{-T}}{1 - \beta + \beta e^{-T}} \tag{9}$$

² This term was introduced by Nusse and Yorke in [8] (see also [9]), and now is widely used in piecewise smooth systems.

³ A scale transformation is a linear transformation that enlarges (increases) or shrinks (diminishes) objects by a scale factor that is the same in all directions. Its parameter is called scale parameter. This means that it plays no role in the dynamics, and the value $\beta \in (0, 1)$ just modifies the size (or scale) of the state variable.

⁴ We recall that interval I is absorbing because in a finite number of iterations the trajectory of any (in our case) initial condition outside I is mapped in I , from which it cannot escape.

Proposition 1. *The map in (4) has a unique fixed point z^* , globally attracting for $\beta e^{-T}/(1 - \beta) < 1$ and repelling for $\beta e^{-T}/(1 - \beta) > 1$. At $\beta e^{-T} = 1 - \beta$ a degenerate flip bifurcation occurs.*

At the value of the degenerate flip bifurcation (DFB for short) of z^* , for $\beta e^{-T}/(1 - \beta) = 1$, the segment $[z_b, \beta + z_b]$ is filled with cycles of period 2, while for $\beta e^{-T}/(1 - \beta) > 1$ only one attracting 2-cycle exists having one periodic point in $z < z_b$ and one in $z > z_b$. The periodic points of the 2-cycle are given by

$$x_R^2 = \frac{1 + a}{1 - ab}, \quad x_L^2 = \frac{1 + b}{1 - ab} \tag{10}$$

that is:

$$z_R^2 = \frac{(1 - \beta)(1 - e^{-T}) + \beta e^{-2T}}{1 - \beta + \beta e^{-2T}}, \quad z_L^2 = \frac{\beta e^{-2T}}{1 - \beta + \beta e^{-2T}} \tag{11}$$

Proposition 2. *For $\beta e^{-T}/(1 - \beta) > 1$ the map in (4) has a unique 2-cycle, with periodic points given in (11), attracting for $\beta e^{-2T}/(1 - \beta) < 1$. At $\beta e^{-2T} = 1 - \beta$ a degenerate flip bifurcation occurs.*

The proof follows immediately from the eigenvalue, given by $\lambda = ab = f'(z_L^2)f'(z_R^2)$, and the 2-cycle is stable as long as $ab > -1$, that is, as long as

$$\frac{\beta e^{-2T}}{1 - \beta} < 1. \tag{12}$$

At $\beta e^{-2T} = 1 - \beta$, when $\lambda = -1$, the 2-cycle also undergoes a DFB (due to the local linearity of the conjugate map (7)). However, now it is not easy to predict what will be the result of this bifurcation, when the 2-cycle becomes unstable. We shall return to this below, making use of the properties of the skew-tent map (7). Taking advantage of this, we know that when the fixed point z^* is unstable the map f can have an attracting cycle q_k of any period $k \geq 2$ (but only with specific symbol sequences, as clarified below) as well as cyclical chaotic intervals Q_k of any period $k \geq 1$. Let us first describe the routes associated with the cycles of period $k \geq 3$, after which we shall describe the effects of the degenerate flip bifurcation of the 2-cycle.

As shown in [6] (see also [2,9,11]), the cycles of the skew-tent map having period $k \geq 3$ appear in pairs,⁵ one of which may be stable or unstable (with the symbol sequence RL^{k-1} , also called principal cycles or maximal cycles), and one always unstable (with the symbol sequence R^2L^{k-2}). Thus, the bifurcation curve, denoted as BCB_k , which corresponds to a “saddle-node” border collision bifurcation, gives rise to a cycle q_k which may be attracting, and to a companion repelling cycle, called q'_k .

In Fig. 2 the two-dimensional bifurcation diagram of the map (7) in the (a, b) -parameter plane is shown in the interesting region (interesting not only for the skew-tent map, but also, as we have remarked above, for the applied model in (4)). The right boundary of the stability region of the cycle, denoted $\Pi(q_k)$, is the curve DFB_k corresponding to the degenerate flip bifurcation of the attracting cycle q_k which becomes repelling, leading to cyclical chaotic intervals of double period, Q_{2k} . All these cycles of period $k \geq 3$ undergo the same bifurcation sequence (increasing the parameter a), that is, the degenerate flip bifurcation $q_k \Rightarrow Q_{2k}$ is followed by the transitions of cyclical chaotic intervals $Q_{2k} \Rightarrow Q_k \Rightarrow Q_1$. The boundary between the region Q_{2k} and the region Q_k is the curve H_k corresponding to the first homoclinic bifurcation of the cycle q_k , while the right boundary of the region Q_k is the curve H'_k related to the first homoclinic bifurcation of the cycle q'_k , leading to a one-piece chaotic interval $Q_1 = I$. We recall that in the skew-tent map the existence of chaotic behavior is persistent under variation of the parameters, so that we have robust chaos, as defined in [1].

In the portion of the parameter plane shown in Fig. 2 only the stability region of the cycle q_3 is observable, but in the strip $a \in (0, 0.5)$ all the regions $\Pi(q_k)$ exist where $k \rightarrow \infty$ as b tends to $-\infty$, and this limit point is relevant also in our application (as we shall see in Fig. 3, corresponding to $\beta = 0.5$ and $T = 0$).

The bifurcation curves can be detected analytically using the coordinates of the points of the cycles.

⁵ We recall that in a continuous map, as it is our case, the appearance of cycles not related to a flip bifurcation always occurs in pair. That is, the bifurcation is similar to a fold bifurcation (or tangent bifurcation) and leads to the existence of two distinct cycles.

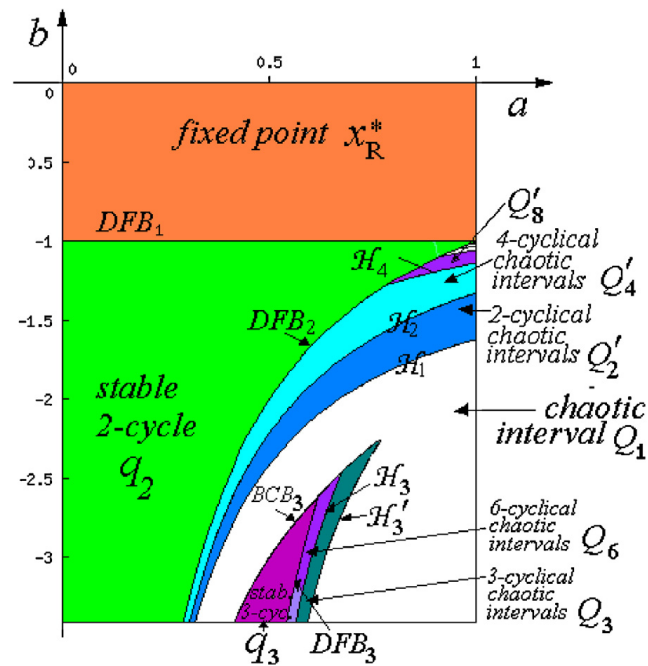


Fig. 2. Two-dimensional bifurcation diagram of the skew-tent map given in (7), in a portion of the (a, b) parameter plane. Robust chaos in one unique interval occurs when the parameters are in the white region.

In order to find the periodic points of such cycles, we consider the periodic point which is the closest to zero on the right side. So by solving the equation $F_L^{k-1} \circ F_R(x_1^{k,s}) = x_1^{k,s}$ we obtain the periodic point $x_1^{k,s}$ of the cycle q_k , which leads to the point

$$x_1^{k,s} = \frac{1 - a^k}{(1 - a)(1 - ba^{k-1})}, \tag{13}$$

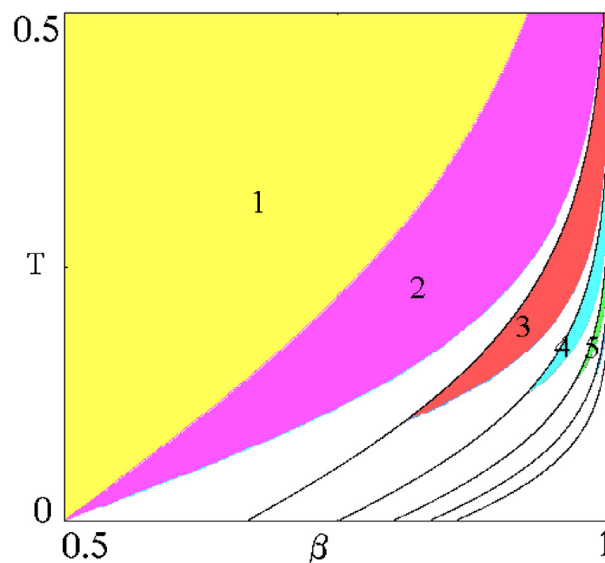


Fig. 3. Two-dimensional bifurcation diagram for $f(z)$ in the parameter plane (β, T) , where $T=T_1=T_2$. The white region corresponds to robust chaotic dynamics.

while the periodic point $x_1^{k,u}$ of the cycle q'_k is obtained by solving the equation $F_L^{k-2} \circ F_R^2(x_1^{k,u}) = x_1^{k,u}$, which leads to the point

$$x_1^{k,u} = \frac{ba^{k-2}(1-a) + 1 - a^{k-1}}{(1-a)(1-b^2a^{k-2})}. \tag{14}$$

The BCB occurs when the periodic point $x_1^{k,u}$ collides with the border, $x_1^{k,u} = 0$, that is, for:

$$BCB_k : \quad b = -\frac{1 - a^{k-1}}{(1-a)a^{k-2}} \tag{15}$$

leading, in terms of the parameters of our model in (4), to:

$$BCB_k : \quad \beta = \frac{1 - e^{-T(k-1)}}{1 - e^{-Tk}}. \tag{16}$$

A sequence of periodicity regions, bounded by the curves given in (16) for $k = 3, \dots, 7$, are shown in Fig. 3.

Thus, when the BCB curve denoted BCB_k is crossed, a pair of cycles appears: q'_k (a periodic point of which is given in (14)), and q_k (a periodic point of which is given in (13)). The cycle q_k is attracting for $b < b_k$, where b_k is defined below, while both cycles are repelling if $b > b_k$. The eigenvalue of the stable cycle q_k is given by $\lambda = ba^{k-1}$ so that it loses stability via degenerate flip bifurcation when $b = -1/a^{k-1}$, that is when:

$$DFB_k : \quad \frac{\beta e^{-T}}{1 - \beta} = \frac{1}{e^{-T(k-1)}} \tag{17}$$

Thus the stability region of the cycle q_k is given by $(a, b) \in \Pi(q_k)$ where

$$\Pi(q_k) = \left\{ (a, b) : -\frac{1}{a^{k-1}} \leq b \leq -\frac{1 - a^{k-1}}{(1-a)a^{k-2}} \right\} \tag{18}$$

that is, in terms of our parameters:

$$\Pi(q_k) : \quad \frac{1}{e^{-T(k-1)}} \geq \frac{\beta e^{-T}}{1 - \beta} \geq \frac{1 - e^{-T(k-1)}}{(1 - e^{-T})e^{T(k-2)}} \tag{19}$$

and it is bounded by the two bifurcation curves BCB_k and DFB_k , which intersect at the point (a_k, b_k) , where a_k is the root of the equation $a^k - 2a + 1 = 0$ in the interval $(0.5, 1)$ and $b_k = -1/a_k^{k-1}$.

So we can state the following

Proposition 3. *The map in (4) has cycles of any period $k \geq 3$ appearing in pairs (q_k and q'_k) at the BCB curves given in (16). The cycle q_k is stable in the region $\Pi(q_k)$ given in (19), and undergoes a degenerate flip bifurcation at the curve DFB_k given in (17).*

The stability region of the fixed point, of the 2-cycle and those of the cycles q_k for $k \geq 3$ are the only regions, in the parameter plane of interest, associated with attracting cycles. In any other point the dynamics are chaotic, and with robust chaos. Moreover, we can analytically determine the qualitative behavior of the chaotic intervals. That is, we can perfectly predict how many bands constitute the chaotic attractor. In fact, we recall that the degenerate flip bifurcation of q_k for $k \geq 3$ leads to cyclical chaotic intervals of double period $2k$, denoted by Q_{2k} . The boundaries of the chaotic interval are always given by the critical point $x = 1$ and its iterates. The attracting $2k$ -cyclical chaotic intervals Q_{2k} exist in the parameter region bounded by the curves BCB_k , DFB_k and by the curve denoted H_k related to the first homoclinic bifurcation of the cycle q_k , given by (see [11])

$$H_k : \quad a^{2(k-1)}b^3 - b + a = 0. \tag{20}$$

The transition $Q_{2k} \Rightarrow Q_k$ (from $2k$ -cyclical to k -cyclical chaotic intervals) takes place crossing the curve H_k , while the transition $Q_k \Rightarrow Q_1$ (from k -cyclical chaotic intervals to a single chaotic interval) occurs crossing the curve denoted H'_k corresponding to the first homoclinic bifurcation of the cycle q'_k , given by

$$H'_k : \quad a^{k-1}b^2 + b - a = 0. \tag{21}$$

It is clear that by making the substitutions $a = e^{-T}$ and $b = -\beta e^{-T}/(1 - \beta)$ in (20) and (21) we obtain the equations of the homoclinic bifurcations in the parameter plane (β, T) of interest for the map in (4), involving the chaotic intervals. These curves of homoclinic bifurcations separate the regions located below the stability regions $\Pi(q_k)$ (given in (19)) shown in Fig. 3, associated with different number of components in the cyclical chaotic intervals, which correspond to true robust chaos.

Now let us consider the 2-cycle. It is possible to see in Fig. 2 that the DFB of the 2-cycle q_2 is particular. The 2-cycle is in fact a particular one because it does not appear by border collision bifurcation (in pairs with a repelling one) as it occurs for the other k -cycles. Instead, as we have seen above, the 2-cycle appears after the degenerate flip bifurcation of the fixed point (occurring at $b = -1$). As we have already seen above, the degenerate flip bifurcation of the 2-cycle of the skew-tent map (7) occurs when $ab = -1$, thus giving the bifurcation curve shown in Fig. 2, which corresponds to $\beta e^{-2T} = 1 - \beta$ in terms of our parameters (from (12)), as shown in Fig. 3. Differently from the cycles q_k for $k \geq 3$ described above, the DFB of the 2-cycle q_2 may lead to m -cyclical chaotic intervals of any even period m . That is, we can have the transition $q_2 \Rightarrow Q'_{2m}$, for any $m \geq 2$, and $m \rightarrow \infty$ as $b \rightarrow -1$ and $a \rightarrow 1$. Two contiguous regions Q'_{2i} and Q'_{2i+1} are separated by the curve corresponding to the first homoclinic bifurcation of the 2^i -cycle, whose equation, of the skew-tent map (7), is given by

$$H_{2^i} : b^{\delta_{i+1}} a^{\delta_i} + (-1)^i (b - a) = 0, \tag{22}$$

where $\delta_m, m = 0, 1, \dots$, are the solutions of the difference equations $\delta_{i+1} = 2\delta_i + (1 + (-1)^i)/2, i = 1, 2, \dots$, with $\delta_0 = 1$ (see [6] for further details).

The bifurcation curve H_1 corresponds to the homoclinic bifurcation of the fixed point $x_R^* = 1/(1 - b)$ occurring when $F^3(0) = 1/(1 - b)$, that is:

$$H_1 : ab^2 + b - a = 0. \tag{23}$$

In our parameters, $a \rightarrow 1$ and $b \rightarrow -1$ correspond to $T \rightarrow 0$ and $\beta \rightarrow 0.5$, that is the lower left corner in Fig. 3. This means that in the white region close to that point, in Fig. 3, we have cyclical chaotic intervals in 2^m pieces for the map in (4), separated by the homoclinic bifurcation curves given in (22) and (23) after the substitutions $a = e^{-T}$ and $b = -\beta e^{-T}/(1 - \beta)$.

3.2. Generic case

Now let us consider the map in (1), with $T_1 \neq T_2$, which is piecewise smooth (instead of piecewise linear). Although it is not possible to detect the fixed point and the other periodic orbits analytically, we only have the same kind of bifurcations which occur in the piecewise linear map. The fixed point undergoes a flip bifurcation and then it leads to chaotic intervals. A sequence of saddle-node bifurcations occur, associated with a pair of k -cycles, for $k \geq 3$, and the stable cycle undergoes a flip bifurcation, which is then followed by chaotic sets. In the 3D parameter space we can detect the analytic equation of the surfaces in which the saddle-node bifurcations of k -cycles occur. To detect this we know that the saddle-node bifurcations are also border collision bifurcations for the point $z = z_b$ so that at the bifurcation of a $(n + 1)$ -cycle we must have $f_L^n \circ f_R(z_b) = z$ and also

$$f_L^{n-1} \circ f_R \circ f_L(z_b) = z_b. \tag{24}$$

This equation can be written in explicit form, in fact, we have

$$f_L^{n-1} \circ f_R \circ f_L(z_b) = f_L^{n-1} \circ f_R(\beta)$$

and using

$$f_L^j(z) = A^j z + (1 - A^j), A = e^{-T_1}$$

we get

$$f_L^{n-1} \circ f_R(\beta) = A^{n-1} f_R(\beta) + (1 - A^{n-1}), A = e^{-T_1}$$

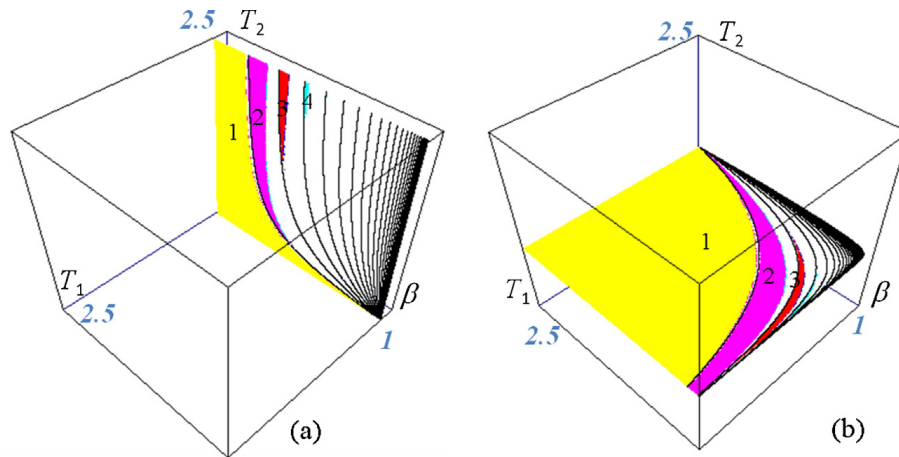


Fig. 4. Two-dimensional sections in the three-dimensional parameter space (T_1, β, T_2) for $f(z)$ in the range $[0, 2.5] \times [0, 1] \times [0, 2.5]$. In (a) at $T_1 = 0.2$. In (b) at $T_2 = 1$. The white region corresponds to chaotic dynamics.

so that the condition in (24) becomes

$$\beta = \frac{1 - e^{-nT_1}}{1 - e^{-T_2}e^{-nT_1}}. \tag{25}$$

Clearly for $T_1 = T_2 = T$, we obtain the same BCB curves already obtained in (16) (noticing that $k = n + 1$). We have thus proved the following proposition:

Proposition 4. *The map in (1) has cycles of any period $k \geq 3$ appearing in pairs $(q_k$ and $q'_k)$ at the BCB curves given in (25).*

A few periodicity regions are shown in Fig. 4, in two sections of the three-dimensional parameter space, where some BCB curves given in (25) for $k \geq 3$ are also shown. The white regions correspond to the existence of robust chaos.

In the generic case, when $T_1 \neq T_2$, the right segment of the map is nonlinear. Hence the flip bifurcation will not be truly degenerate. However, the curvature in this case is very small so that the character of the bifurcation will be almost like a degenerate bifurcation. As an example, we show in Fig. 5 two one-dimensional bifurcation diagrams, reporting the state variable z as a function of the parameter β . Fig. 5(a) shows the bifurcation diagram for the symmetric case ($T_1 = T_2 = T$), while Fig. 5(b) shows an example in the generic case ($T_1 \neq T_2$). This shows that the analytical results obtained for the simpler piecewise linear map give reasonably accurate description of the behavior of the actual system.

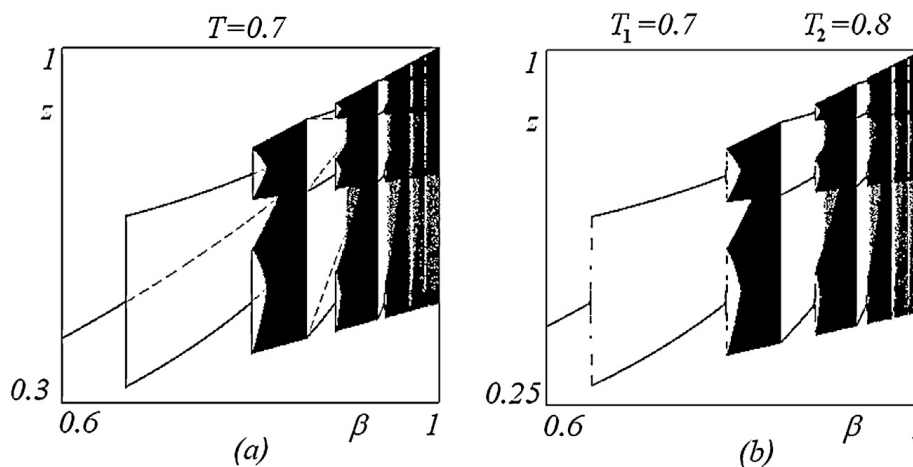


Fig. 5. One-dimensional bifurcation diagram for $f(z)$ showing z as a function of β . In (a) in the symmetric case for $T_1 = T_2 = 0.7$. In (b) in the generic case for $T_1 = 0.7$ and $T_2 = 0.8$.

4. Conclusions

In this work we have considered a system proposed as chaos generator in [7]. For such a chaotic system, used for practical application, a complete bifurcation analysis becomes quite important, in order to predict its behavior in different parameter regimes. This objective has been reached in the particular case $T_1 = T_2 = T$, considered in Section 3.1. Under this assumption the piecewise smooth one-dimensional map reduces to a piecewise linear one, which is topologically conjugated with the skew tent map. Making use of the theory already developed for the skew-tent map, we have obtained the parameter domains of different dynamical behaviors for the inductorless chaos generator in the symmetric case, showing all the regions in the parameter plane which are associated with attracting cycles or to robust chaos in cyclic chaotic intervals.

In the generic case, the border collision bifurcations leading to the appearance of a pair of k -cycles, $k \geq 3$, have been analytically detected in Section 3.2. By numerical evidence, we conjecture that the sequence of bifurcations occurring in the general model are of the same kind, and lead to robust chaos.

References

- [1] S. Banerjee, J.A. Yorke, C. Grebogi, Robust chaos, *Physical Review Letters* 80 (1998) 3049–3052.
- [2] S. Banerjee, M.S. Karthik, G. Yuan, J.A. Yorke, Bifurcations in one-dimensional piecewise smooth maps. Theory and applications in switching circuits, *IEEE Transactions on Circuits and Systems I* 47 (2000) 389–394.
- [3] L.O. Chua, The genesis of Chua's circuit, *Archiv fur Elektronik und Ubertragungstechnik* 46 (1992) 250–257.
- [4] L.O. Chua, Chua's circuit 10 years later, *International Journal of Circuit Theory and Applications* 22 (1994) 279–305.
- [5] S. Ito, S. Tanaka, H. Nakada, On unimodal transformations and chaos II, *Tokyo Journal of Mathematics* 2 (1979) 241–259.
- [6] Y.L. Maistrenko, V.L. Maistrenko, L.O. Chua, Cycles of chaotic intervals in a time-delayed Chua's circuit, *International Journal of Bifurcation and Chaos* 3 (1993) 1557–1572.
- [7] S. Mandal, S. Banerjee, Analysis and CMOS implementation of a chaos-based communication system, *IEEE Transactions on Circuits and Systems I* 51 (2004) 1708–1722.
- [8] H.E. Nusse, J.A. Yorke, Border-collision bifurcations including period two to period three for piecewise smooth systems, *Physica D* 57 (1992) 39–57.
- [9] H.E. Nusse, J.A. Yorke, Border-collision bifurcation for piecewise smooth one-dimensional maps, *International Journal of Bifurcation and Chaos* 5 (1995) 189–207.
- [10] J.C. Sprott, Simple chaotic systems and circuits, *American Journal of Physics* 68 (2000) 758–763.
- [11] I. Sushko, L. Gardini, Degenerate bifurcations and border collisions in piecewise smooth 1D and 2D maps, *International Journal of Bifurcation and Chaos* 20 (2010) 2045–2070.
- [12] F. Takens, Transitions from periodic to strange attractors in constrained equations, in: M.I. Camacho, M.J. Pacifico, F. Takens (Eds.), *Dynamical Systems and Bifurcation Theory*, Research Notes in Mathematics Series, 160, Longman Scientific and Technical, Pitman, 1987, pp. 399–421.